

# COMPUTATIONAL INVESTIGATIONS OF AN INTERNALLY HEATED CONVECTIVE-RADIATIVE POROUS FIN SUBJECTED TO MAGNETIC FIELD: COMPARATIVE METHODS AND PARAMETRIC STUDIES

M. G. SOBAMOWO<sup>1,\*</sup>, A. A. YINUSA<sup>1</sup>, H. BERREHAL<sup>2</sup>, R. O. OLA-GBADAMOSI<sup>3</sup>, M. O. SALAMI<sup>1</sup>, E. H. ABUBAKAR<sup>4</sup>, S. A. OLADOSU<sup>3</sup>

<sup>1</sup>Department of Mechanical Engineering, University of Lagos, Akoka, Lagos, Nigeria

<sup>2</sup>Department of Physics, University of Brothers Mentouri Constantine 1, Algeria

<sup>3</sup>Department of Mechanical Engineering, Lagos State University, Epe Campus, Lagos, Nigeria

<sup>4</sup>Department of Civil and Environmental Engineering, University of Lagos, Akoka, Lagos, Nigeria

\*Corresponding Author: M. G. SOBAMOWO (Email: mikegbeminiyiprof@yahoo.com)

(Received: 12-Oct-2022; accepted: 24-Feb-2023; published: 31-Mar-2023)

DOI: <http://dx.doi.org/10.55579/jaec.202371.391>

**Abstract.** *The concern of this paper is to compare the computational efficiencies and accuracies of three approximate analytical methods; namely, homotopy analysis method (HAM), optimal homotopy asymptotic method (OHAM) and differential transform method (DTM) for the nonlinear thermal performance analysis of a convective-radiative porous fin with temperature-dependent internal heat generation under the influence of the magnetic field. To establish the computational accuracies of the three methods, the results of the three-series solutions are compared with the results of the developed exact analytical and numerical methods. Also, the symbolic solutions developed in this work are used to explore the impacts of the controlling parameters on the performance of the passive device. It is established that as the conductive-convective, conductive-radiative and magnetic field parameters increase, the fin temperature distribution decreases and hence, the fin thermal efficiency is improved. An increase in temperature distribution in the fin is noticed as the nonlinear thermal conductivity parameter increases. It is envisaged that the present study will give a good insight into the*

*nonlinear analysis of extended surfaces which will aid proper design in thermal systems.*

## Keywords

*Approximate analytical methods, rectangular porous fin, nonlinear analysis, comparative and parametric studies.*

## 1. Introduction

The non-expensive but effective cooling of electronics and thermal systems have been achieved through the applications of passive devices such as fins [1]. The importance of extended surfaces has incited a large number of research in literatures. The theoretical investigations of thermal damage problems and heat transfer enhancement by the extended surfaces have attest to facts that the controlling thermal models for the passive devices are usually nonlinear. Consequently, the nonlinear thermal models have been successfully analyzed in the past studies with the aids of approximate analytical, semi-

analytical, semi-numerical, and numerical methods [2, 3, 4, 5, 6, 7]. In such previous studies, Jordan et al. [8] adopted optimal linearization method to solve the nonlinear problems in the fin while Kundu and Das [9] utilized Frobenius expanding series method for the analysis of the nonlinear thermal model. Subsequently, Khani et al. [10] and Amirkolaei and Ganji [11] applied homotopy analysis method to analyze and obtain fin thermal profiles. In a further analysis, Aziz and Bouaziz [12], Sobamowo [13], Ganji et al. [14] and Sobamowo et al. [15] employed methods of weighted residual to explore the nonlinear thermal behaviour of fins. In another studies, methods of double decomposition and variation of parameter were used by Sobamowo [16] and Sobamowo et al. [17], respectively to study the thermal characteristics of fins. Also, differential transformation method has been used by some researchers such as Moradi and Ahmadikia [18], Sadri et al. [19], Ndlovu and Moitsheki [20], Mosayebidarchech et al. [21], Ghasemi et al. [22] and Ganji and Dogonchi [23] to predict the heat transfer behaviour in passive devices. With the help of homotopy perturbation method, Sobamowo et al. [24], Arslanturk [25], Ganji et al. [26] and Hoshyar et al. [27] scrutinized the heat flow in the extended surfaces. However, these studies are for thermal analysis of fin under assumed constant heat transfer coefficient. The cases of heat transfer with variable heat transfer coefficient along the passive device have also been investigated [28, 29, 30, 31, 32, 33, 34, 35]. Such analysis helps in providing the needed information on the efficiency, effectiveness, and design of the extended surfaces under various boiling modes [33, 34, 35, 36, 37, 38, 39, 40, 41, 42, 43, 44].

In most engineering materials, the thermal conductivities of fin materials are temperature-dependent, the influence of the temperature-dependent thermal properties on the performance of fin have been explored in past studies. However, Sobamowo et al; [45] presented some figures that show that the thermal conductivity of palladium is constant at a relatively low temperature. This depicts that the thermal performances of some materials have temperature-invariant thermal conductivity within some ranges of temperature. More-

over, influence of Lorentz force and temperature-variant internal heat generation on the temperature distribution of the extended surfaces is yet to be analyzed using optimal asymptotic analysis and homotopy analysis methods. The analytical approaches of these methods reduce the complex mathematical analysis, high computational cost and time. Furthermore, under large values of thermo-geometric and nonlinear thermal conductivity parameters, it is established that applications of Adomian decomposition and homotopy perturbation methods are limited [46]. However, through a holistic assumed exponential solution in optimal asymptotic method and an inherent property of auxiliary parameters for the adjustment and control of region and rate of convergence of approximate series solutions, homotopy analysis method has proven to be an efficient and capable technique in handling nonlinear engineering problems in wider ranges of parameters. Therefore, the present work compares the computational efficiencies and accuracies of three approximate analytical methods, namely, homotopy analysis method, optimal homotopy asymptotic method and differential transformation method for the nonlinear thermal performance analysis of a convective-radiative porous fin with temperature-dependent internal heat generation under the influence of magnetic field. The developed symbolic solutions are used to explore the influences of the controlling thermal model parameters on the performance of the fin.

## 2. Problem formulation

In Fig. 1, it is consideration is given to a porous fin with temperature-invariant thermal properties allowing radiative and convective heat transfer.

To thermally describe the behaviour of the passive device, assumptions are made that the porous medium is filled with fluid of single-phase. The solid portion of the extended surface is homogeneous and isotropic. The fin temperature changes only along its length and the condition of a perfect thermal contact between the prime surface and the fin base is assumed.

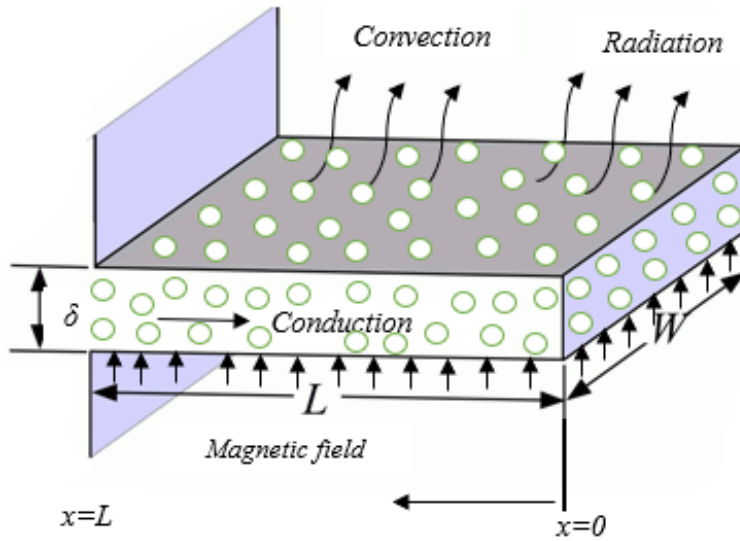


**Fig. 1:** Schematic of convective-radiative longitudinal fin under even magnetic field.

From the assumptions and with the aid of Darcy’s model, the energy balance is

Expansion of the first term in Eq. (1), it provides

$$\begin{aligned}
 \frac{d}{d\tilde{x}} \left( \frac{d\tilde{T}}{d\tilde{x}} + \frac{4\sigma}{3k_{eff}\beta_R} \frac{d\tilde{T}^4}{d\tilde{x}} \right) & - \frac{\rho\beta c_p g K}{vk_{eff}A_{cr}} (\tilde{T} - T_a)^2 \\
 & - \frac{h(1-\varepsilon)P}{k_{eff}A_{cr}} (\tilde{T} - T_a) \\
 & - \frac{\sigma P \in}{k_{eff}A_{cr}} (\tilde{T}^4 - T_a^4) \\
 & - \frac{\mathbf{J}_c \times \mathbf{J}_c}{\sigma k_{eff}A_{cr}} A_s + \frac{q(\tilde{T})}{k_{eff}} = 0
 \end{aligned} \tag{1}$$

The boundary conditions are

$$\begin{aligned}
 \tilde{x} = 0, & \tag{3a} \\
 \frac{d\tilde{T}}{d\tilde{x}} = 0, &
 \end{aligned}$$

$$\begin{aligned}
 \tilde{x} = L, & \tag{3b} \\
 \tilde{T} = T_b &
 \end{aligned}$$

The internal heat general varies linearly with temperature as Therefore,

$$q(\tilde{T}) = q_a \left( 1 + \lambda (\tilde{T} - T_a) \right) \quad (4)$$

When Eq. (4) is substituted into Eq. (2), one arrives at

$$\begin{aligned} \frac{d^2\tilde{T}}{d\tilde{x}^2} + \frac{4\sigma}{3k_{eff}\beta_R} \frac{d}{d\tilde{x}} \left( \frac{d\tilde{T}^4}{d\tilde{x}} \right) \\ - \frac{\rho\beta c_p g K}{v\delta k_{eff}} (\tilde{T} - T_a)^2 \\ - \frac{h(1-\varepsilon)}{k_{eff}\delta} (\tilde{T} - T_a) \\ - \frac{\sigma \in}{k_{eff}\delta} (\tilde{T}^4 - T_a^4) - \frac{\mathbf{J}_c \times \mathbf{J}_c}{\sigma k_{eff} A_{cr}} A_s \\ + \frac{q_o}{k_{eff}} \left( 1 + \lambda (\tilde{T} - T_a) \right) = 0 \end{aligned} \quad (5)$$

The radiative temperature term can be expressed as a linear function of temperature as

$$\begin{aligned} \tilde{T}^4 = T_a^4 + 4T_a^3 (\tilde{T} - T_a) \\ + 6T_a^2 (\tilde{T} - T_a)^2 + \dots \\ \cong 4T_a^3 \tilde{T} - 3T_a^4 \end{aligned} \quad (6)$$

Substitution of Eq. (6) into Eq. (5), results in

$$\begin{aligned} \frac{d^2\tilde{T}}{d\tilde{x}^2} + \frac{16\sigma}{3k_{eff}\beta_R} \frac{d^2\tilde{T}}{d\tilde{x}^2} \\ - \frac{\rho\beta c_p g K}{v\delta k_{eff}} (\tilde{T} - T_a)^2 \\ - \frac{h(1-\varepsilon)}{k_{eff}\delta} (\tilde{T} - T_a) \\ - \frac{4\sigma T_a^3 \in}{k_{eff}\delta} (\tilde{T} - T_a) - \frac{\mathbf{J}_c \times \mathbf{J}_c}{\sigma k_{eff} A_{cr}} A_s \\ + \frac{q_o}{k_{eff}} \left( 1 + \lambda (\tilde{T} - T_a) \right) = 0 \end{aligned} \quad (7)$$

It should be noted that

$$\frac{\mathbf{J}_c \times \mathbf{J}_c}{\sigma} = \sigma_m B_o^2 u^2 \quad (8)$$

$$\begin{aligned} \frac{d^2\tilde{T}}{d\tilde{x}^2} + \frac{16\sigma}{3k_{eff}\beta_R} \frac{d^2\tilde{T}}{d\tilde{x}^2} \\ - \frac{\rho\beta c_p g K}{v\delta k_{eff}} (\tilde{T} - T_a)^2 \\ - \frac{h(1-\varepsilon)}{k_{eff}\delta} (\tilde{T} - T_a) \\ - \frac{\sigma T_a^3 \in}{k_{eff}\delta} (\tilde{T} - T_a) - \frac{\sigma_m B_o^2 u^2}{A_{cr} k_{eff}} A_s \\ + \frac{q_o}{k_{eff}} \left( 1 + \lambda (\tilde{T} - T_a) \right) = 0 \end{aligned} \quad (9)$$

Applying the following adimensional parameters in Eq. (10) to Eq. (9),

$$X = \frac{\tilde{x}}{L}, \quad \theta = \frac{\tilde{T} - T_a}{T_b - T_a}, \quad S_h = \frac{\rho\beta c_p g K}{k_{eff}\delta v} L^2,$$

$$M^2 = \frac{h(1-\varepsilon)L^2}{k_{eff}t}, \quad Rd = \frac{4\sigma_{st}T_\infty^3}{3\beta_R k_{eff}},$$

$$N = \frac{4\sigma_{st} \in L^2 T_\infty^3}{k_{eff}t}.$$

$$Ha = \frac{\sigma A_s B_o^2 u^2 L^2}{A_{cr} k_{eff}}, \quad G = \frac{q_o t}{h(T_L - T_\infty)}, \quad (10)$$

$$\gamma = \lambda(T_b - T_a)$$

One arrives at the adimensional form of the governing Eq. (9) as presented in Eq. (11),

$$\begin{aligned} \frac{d^2\theta}{dX^2} + 4Rd \frac{d^2\theta}{dX^2} - S_h \theta^2 - M^2 \theta \\ - N\theta - Ha + M^2 G (1 + \gamma\theta) = 0 \end{aligned} \quad (11)$$

and the adimensional boundary conditions

$$X = 0, \quad (12a)$$

$$\frac{d\theta}{dX} = 0$$

$$X = 1, \quad (12b)$$

$$\theta = 1$$

Eq. (11) can be written as

$$\begin{aligned} \frac{d^2\theta}{dX^2} - \frac{S_h}{1+4Rd}\theta^2 - \frac{M^2}{1+4Rd}\theta \\ - \frac{N}{1+4Rd}\theta - \frac{Ha}{1+4Rd} \\ + \frac{M^2G}{1+4Rd}(1+\gamma\theta) = 0 \end{aligned} \tag{13}$$

Taking

$$\begin{aligned} Mc^2 = \frac{M^2}{1+4Rd}, \quad Nr = \frac{N}{1+4Rd}, \tag{14} \\ Ra = \frac{S_h}{1+4Rd}, \quad H = \frac{Ha}{1+4Rd}, \quad Q = \frac{G}{1+4Rd}, \end{aligned}$$

we arrived at the dimensionless forms of the governing as follows;

$$\begin{aligned} \frac{d^2\theta}{dX^2} - Ra\theta^2 - Mc^2\theta - Nr\theta \\ - H + Mc^2Q + Mc^2Q\gamma\theta = 0 \end{aligned} \tag{15}$$

and the dimensionless boundary conditions still remain the same as in Eqs. (12).

### 3. Application of Homotopy Analysis Method to the Nonlinear Thermal Problem

It can be seen that the above governing differential equation is highly nonlinear, and such nonlinearity imposes some difficulties in the development of exact analytical methods to generate closed form solution for the equation. Therefore, homotopy analysis method is presented in this work. The homotopy analysis method (HAM) which is an analytical scheme for providing approximate solutions to ordinary differential equations is adopted in generating solutions to ordinary nonlinear differential equations. Upon constructing the homotopy, the initial guess and auxiliary linear operator can be

expressed as

$$\theta_0(X) = 1 \tag{16}$$

$$L(\theta) = \theta'' \tag{17}$$

$$L(c_1X + c_2) = 0 \tag{18}$$

Where  $c_i (i = 1, 2, 3, 4)$  are constants. Let  $P = \in [0, 1]$  denotes the embedding parameter and  $\hbar$  is the non-zero auxiliary parameter. Therefore, the homotopy is constructed as

#### 3.1. Zeroth-order deformation equations

$$\begin{aligned} (1-p)L[\theta(X;p) - \theta_0(X)] \\ = p\hbar H(X)N[\theta(X;p)] \end{aligned} \tag{19}$$

$$\theta'(0;p) = 0; \quad \theta(1;p) = 1; \tag{20}$$

when  $p = 0$  and  $p = 1$  we have

$$\theta(X;0) = \theta_0(X); \quad \theta(X;1) = \theta(X) \tag{21}$$

As  $p$  increases from 0 to 1.  $\theta(X;p)$  varies from  $\theta_0(X)$  to  $\theta(X)$ . By Taylor's theorem and utilizing Eq. (20),  $\theta(X;p)$  can be expanded in the power series of  $p$  as follows:

$$\theta(X;p) = \theta_0(X) + \sum_{m=1}^{\infty} \theta_m(X)p^m, \tag{22}$$

$$\theta_m(X) = \frac{1}{m!} \left. \frac{\partial^m(\theta(X;p))}{\partial p^m} \right|_{p=0}$$

where  $\hbar$  is chosen such that the series is convergent at  $p = 1$ ; therefore, by Eq. (22) it is easily shown that

$$\theta(X) = \theta_0(X) + \sum_{m=1}^{\infty} \theta_m(X) \tag{23}$$

#### 3.2. m-th order deformation equations

$$L[\theta_m(\eta) - \chi_m\theta_{m-1}(\eta)] = \hbar H(X)R_m(X) \tag{24}$$

$$\theta'(0;p) = 0; \quad \theta(1;p) = 0 \tag{25}$$

where

$$R_m(X) = \frac{d^2\theta(X;p)}{dX^2} - Sh \sum_{i=0}^{n-1} \theta_{n-1-k}\theta_k \quad (26)$$

$$- Mc^2\theta_{n-1} - Nr\theta_{n-1} - Ha$$

$$+ Mc^2Q + Mc^2Q\gamma\theta_{n-1}$$

Now the results for the convergence, differential equation and the auxiliary function are determined according to the solution expression. Assuming;

$$H(X) = 1 \quad (27)$$

The analytic solution is developed using the MATLAB computational stencil. Hence, the first deformation is expressed below

$$\theta_1(X) = \frac{1}{2}\hbar(-Ra - Mc^2 + Mc^2Q + Mc^2Q\gamma$$

(28)

$$- H) X^2 + \frac{1}{2}\hbar Ra + \frac{1}{2}\hbar Mc^2$$

$$- \frac{1}{2}\hbar Mc^2Q - \frac{1}{2}\hbar Mc^2Q\gamma + \frac{1}{2}\hbar H$$

$$\theta_2(X) = \frac{5}{120}\hbar^2(-Ra - Mc^2 + Mc^2Q + Mc^2Q\gamma$$

$$- H) (-2Ra - Mc^2 + M^2Q\gamma) X^4$$

$$+ \frac{1}{2} \left[ -\hbar Ra - \hbar Mc^2 + \hbar Mc^2Q - \hbar H$$

$$+ \frac{3}{2}\hbar^2 RaMc^2Q\gamma - \hbar^2 Ra - \hbar^2 Mc^2$$

$$- \hbar^2 Ra^2 - \frac{1}{2}\hbar^2 Mc^4 + \hbar^2 Mc^2Q - \hbar^2 H$$

$$- \frac{3}{2}\hbar^2 RaMc^2 + \frac{1}{2}\hbar^2 Mc^4Q$$

$$- \frac{1}{2}\hbar^2 Mc^2H + \hbar^2 RaMc^2Q - \hbar^2 RaH$$

$$+ \hbar^2 Mc^4Q\gamma + \hbar Mc^2Q\gamma$$

$$- \frac{1}{2}\hbar^2 Mc^4Q^2\gamma + \frac{1}{2}\hbar^2 HMc^2Q\gamma$$

$$- \frac{1}{2}\hbar^2 Mc^4Q^2\gamma^2 + \hbar^2 Mc^2Q\gamma \Big] X^2$$

$$+ \frac{5}{24}\hbar^2 Mc^4 - \frac{1}{2}\hbar^2 Mc^2Q + \frac{5}{8}\hbar^2 Mc^2$$

$$- \frac{5}{24}\hbar^2 Mc^4Q + \frac{5}{24}\hbar^2 Mc^2H + \frac{1}{2}\hbar Mc^2$$

$$+ \frac{5}{24}\hbar^2 Mc^4Q^2\gamma^2 - \frac{5}{12}\hbar^2 RaMc^2Q$$

$$+ \frac{5}{12}\hbar^2 RaH - \frac{5}{12}\hbar^2 Mc^4Q\gamma$$

$$+ \frac{5}{12}\hbar^2 Mc^4Q^2\gamma - \frac{1}{2}\hbar^2 Mc^2Q\gamma$$

$$- \frac{1}{2}\hbar Mc^2Q\gamma - \frac{1}{2}\hbar Mc^2Q + \frac{1}{2}\hbar^2 H$$

$$- \frac{5}{8}\hbar^2 RaMc^2Q\gamma + \frac{1}{2}\hbar^2 Ra$$

$$+ \frac{1}{2}\hbar^2 Mc^2 + \frac{1}{2}\hbar Ra + \frac{5}{12}\hbar^2 Ra^2$$

(29)

Similarly  $\theta_3(\eta), \theta_4(\eta), \theta_5(\eta) \dots$  are found but they are too large expressions that cannot be included in this paper. However, they are included in the results displayed graphically. From the principle of HAM

$$\theta(X) = \theta_0(X) + \sum_{m=1}^{\infty} \theta_m(X) \quad (30)$$

$$= \theta_0(X) + \theta_1(X) + \theta_2(X) + \dots$$

Therefore, substitute Eqs. (16), (28) and 29) into Eq. (30), we have

$$\begin{aligned}
 \theta(X) = & 1 + \frac{1}{2}\hbar(-Ra - Mc^2 + Mc^2Q + Mc^2Q\gamma \\
 & - H) X^2 + \frac{1}{2}\hbar Ra + \frac{1}{2}\hbar Mc^2 \\
 & - \frac{1}{2}\hbar Mc^2Q - \frac{1}{2}\hbar Mc^2Q\gamma + \frac{1}{2}\hbar H \\
 & + \frac{5}{120}\hbar^2(-Ra - Mc^2 + Mc^2Q + Mc^2Q\gamma \\
 & - H)(-2Ra - Mc^2 + M^2Q\gamma) X^4 \\
 & + \frac{1}{2}\left[-\hbar Ra - \hbar Mc^2 + \hbar Mc^2Q - \hbar H \right. \\
 & \quad + \frac{3}{2}\hbar^2 Ra Mc^2 Q\gamma - \hbar^2 Ra - \hbar^2 Mc^2 \\
 & \quad - \hbar^2 Ra^2 - \frac{1}{2}\hbar^2 Mc^4 + \hbar^2 Mc^2Q - \hbar^2 H \\
 & \quad - \frac{3}{2}\hbar^2 Ra Mc^2 + \frac{1}{2}\hbar^2 Mc^4Q \\
 & \quad - \frac{1}{2}\hbar^2 Mc^2H + \hbar^2 Ra Mc^2Q - \hbar^2 RaH \\
 & \quad + \hbar^2 Mc^4Q\gamma + \hbar Mc^2Q\gamma - \frac{1}{2}\hbar^2 Mc^4Q^2\gamma \\
 & \quad \left. + \frac{1}{2}\hbar^2 H Mc^2Q\gamma - \frac{1}{2}\hbar^2 Mc^4Q^2\gamma^2 \right. \\
 & \quad \left. + \hbar^2 Mc^2Q\gamma\right] X^2 \\
 & + \frac{5}{24}\hbar^2 Mc^4 - \frac{1}{2}\hbar^2 Mc^2Q + \frac{5}{8}\hbar^2 Mc^2 \\
 & - \frac{5}{24}\hbar^2 Mc^4Q + \frac{5}{24}\hbar^2 Mc^2H \\
 & + \frac{1}{2}\hbar Mc^2 + \frac{5}{24}\hbar^2 Mc^4Q^2\gamma^2 \\
 & - \frac{5}{12}\hbar^2 Ra Mc^2Q + \frac{5}{12}\hbar^2 RaH \\
 & - \frac{5}{12}\hbar^2 Mc^4Q\gamma + \frac{5}{12}\hbar^2 Mc^4Q^2\gamma \\
 & - \frac{1}{2}\hbar^2 Mc^2Q\gamma - \frac{1}{2}\hbar Mc^2Q\gamma - \frac{1}{2}\hbar Mc^2Q \\
 & + \frac{1}{2}\hbar^2 H - \frac{5}{8}\hbar^2 Ra Mc^2Q\gamma + \frac{1}{2}\hbar^2 Ra \\
 & + \frac{1}{2}\hbar^2 Mc^2 + \frac{1}{2}\hbar Ra + \frac{5}{12}\hbar^2 Ra^2 + \dots
 \end{aligned} \tag{31}$$

### 3.3. Convergence of the HAM solution

In order to control the convergence rate of  $\hbar$  in the approximate analytical solutions given by

HAM, Liao [47] presented the auxiliary parameter. It is established that the convergence rate of approximation for the HAM solution strongly depend on the value of the auxiliary parameter. For the 10th-order of approximation, different values of the model parameters are used for the different simulations to arrive at the acceptable range of values of the parameter  $\hbar$  for the difference controlling parameters of the model.

## 4. Solution of the Thermal Model using Optimal Asymptotic Homotopy Method

The approximate analytical solution of the non-linear thermal model using optimal homotopy asymptotic method is presented in this section.

For OHAM (developed by Marinca and Herizanu [23, 34] and applied in other works [25, 26, 27, 28], we choose the linear operators from Eq. (4) in the form:

$$L[\theta] = \frac{d^2\theta}{dX^2} \tag{32}$$

The initial approximation  $\theta_0(X)$  can be obtain as:

$$\frac{d^2\theta_0}{dX^2} = 0 \tag{33}$$

with the boundary conditions:

$$X = 0, \frac{d\theta_0}{dX} = 0 ; X = 1, \theta_0 = 1 \tag{34}$$

Last equation has solutions:

$$\theta_0(X) = 1 \tag{35}$$

Nonlinear operators corresponding to Eq. (15) and linear operator given in Eq. (35) is defined by:

$$N[\theta] = -\alpha\theta^2(X) - \beta\theta(X) - \lambda \tag{36}$$

where

$$\alpha = Ra, \quad \beta = Mc^2 + Nr - Mc^2Q\gamma,$$

$$\lambda = Ha - Mc^2Q$$

By substituting Eq. (10) into Eq. (11), we can obtain the expression of  $N[\theta_0(X)]$ :

$$N[\theta_0(X)] = -\alpha - \beta - \lambda \tag{37}$$

If we consider the first-order approximate solution for nonlinear differential equation (15):

$$\theta(X) = \theta_0(X) + \theta_1(X, C_i) \tag{38}$$

where  $\theta_1(X, C_i)$  are obtained as:

$$\frac{d^2\theta_1}{dX^2} = N[\theta_0(X)] \hbar(X, C_i) \tag{39}$$

with boundary conditions:

$$X = 0, \frac{d\theta_1}{dX} = 0 ; X = 1, \theta_1 = 0 \tag{40}$$

Note that the convergence of the approximate solution  $\theta(X)$  depends up on the auxiliary function  $\hbar(X, C_i)$ , we can choose  $\hbar(X, C_i)$  as:

$$\hbar(X, C_i) = C_1 + C_2e^{-X} + C_3e^{-2X} + \dots + C_p e^{-(p-1)X} \tag{41}$$

By solving Eq. (39) with boundary condition (40), we obtained:

$$\theta_1(X) = \frac{1}{2}(\beta + \alpha + \lambda) \left\{ \begin{aligned} &\frac{2}{9}C_4(e^{-3X} - e^{-3}) + \frac{1}{2}C_3(e^{-2X} - e^{-2}) + 2C_2(e^{-X} - e^{-1}) \\ &+ (X-1)\left(C_1X + C_1 + 2C_2 + C_3 + \frac{2}{3}C_4\right) \end{aligned} \right\} \tag{42}$$

Finally, the solution (13) is obtained through (10) and (17):

$$\theta(X) = 1 + \frac{1}{2}(\beta + \alpha + \lambda) \left\{ \begin{aligned} &\frac{2}{9}C_4(e^{-3X} - e^{-3}) + \frac{1}{2}C_3(e^{-2X} - e^{-2}) + 2C_2(e^{-X} - e^{-1}) \\ &+ (X-1)\left(C_1X + C_1 + 2C_2 + C_3 + \frac{2}{3}C_4\right) \end{aligned} \right\} \tag{43}$$

Where  $C_i$  is unknown parameters which can be obtained with Least-square method (LSM). In our study we choose  $p = 4$ . For example, when  $Ra=0.3$ ,  $Rd=0.4$ ,  $Nc=0.3$ ,  $Nr=0.5$ ,  $Ha=0.6$ ,  $Q=0$  and  $\varepsilon$ , the values of constants are:  $C1=-3.034900727$ ,  $C2=6.159911506$ ,  $C3=-6.848991138$ ,  $C4=2.590773069$

Substituting these values in Eq. (32), we obtain  $\theta(X)$  in a series form as follow:

$$\theta(X) = 2.652103740 - 2.463964602e^{-X} + 0.6848991138e^{-2X} - 0.1151443183e^{-3X} - 1.439594147X + 0.6069801454X^2 \tag{44}$$

## 5. Differential Transform Method to the Nonlinear Thermal Model

The nonlinear thermal model is also solved in this section using differential transform method. The definition and the operational properties of the method can be found in our previous study [28]. The recursive relations of Eq. (15) is given as

$$(k+1)(k+2)\theta(k+2) - Ra \sum_{l=0}^k \theta(l)\theta(k-l) - Mc^2\theta(k) + Mc^2Q\gamma\theta(k) + (Mc^2Q - H)\delta(k) = 0 \tag{45}$$

where

$$\theta(k+2) = \frac{Ra \sum_{l=0}^k \theta(l)\theta(k-l) + Mc^2\theta(k) - Mc^2Q\gamma\theta(k) - (Mc^2Q - H)\delta(k)}{(k+1)(k+2)} \tag{46}$$

From the boundary conditions, one gets

$$\theta(0) = a, \theta(1) = 0$$

We arrived at

$$\theta(2) = \frac{a^2Ra + aMc^2 - aMc^2Q\gamma - (Mc^2Q - H)}{2}$$

$$\theta(3) = 0$$

$$\theta(4) = \left\{ \frac{2aRa + Mc^2 + Nr - Mc^2Q\gamma}{12} \right\} \left\{ \frac{a^2Ra + aMc^2 - aMc^2Q\gamma - (Mc^2Q - H)}{2} \right\}$$

$$\theta(5) = 0$$

$$\begin{aligned} \theta(6) &= \frac{1}{720} (2aRa + Mc^2 + Nr - Mc^2Q\gamma)^2 \{a^2Ra + aMc^2 - aMc^2Q\gamma - (Mc^2Q - H)\} \\ &+ \frac{1}{120} \{a^2Ra + aMc^2 - aMc^2Q\gamma - (Mc^2Q - H)\}^2 Ra \end{aligned}$$

Therefore, from the definition

$$\begin{aligned} \theta(X) &= a + \left\{ \frac{a^2Ra + aMc^2 + aNr - aMc^2Q\gamma - (Mc^2Q - H)}{2} \right\} X^2 \\ &+ \frac{1}{24} (2aRa + Mc^2 + Nr - Mc^2Q\gamma) \{a^2Ra + aMc^2 + aNr - aMc^2Q\gamma - (Mc^2Q - H)\} X^4 \\ &+ \frac{1}{720} \left[ (2aRa + Mc^2 + Nr - Mc^2Q\gamma)^2 \{a^2Ra + aMc^2 - aMc^2Q\gamma - (Mc^2Q - H)\} \right. \\ &\left. + 6\{a^2Ra + aMc^2 - aMc^2Q\gamma - (Mc^2Q - H)\}^2 Ra \right] X^6 + \dots \end{aligned} \tag{47}$$

## 6. Numerical Procedure for the Steady State Analysis

$$\begin{aligned} p' &= S_h\theta^2 + Mc^2\theta + Nr\theta \\ &+ Ha - Mc^2Q - Mc^2Q\gamma\theta \end{aligned} \tag{49}$$

In order to verify the results of the present work, the nonlinear model in Eq. (15) was also solved numerically using fifth-order Runge-Kutta Fehlberg method (Cash-Karp Runge-Kutta) coupled with shooting method. Since Runge-Kutta method is for solving first-order ordinary differential equation, the fourth-order ordinary differential equation is decomposed into a system of first-order differential equations as follows:

$$\theta(5) = 0 \Rightarrow \theta'' = p', \tag{48}$$

The above Eqs. (48) and (49) can be written as

$$f(X, \theta, p) = p, \tag{50}$$

$$\begin{aligned} g(X, \theta, p) &= S_h\theta^2 + Mc^2\theta + Nr\theta + Ha \\ &- Mc^2Q - Mc^2Q\gamma\theta, \end{aligned}$$

The iterative scheme of the fifth-order Runge-Kutta Fehlberg method (Cash-Karp Runge-Kutta) for the above system of first-order equa-

tions is given as

$$\theta_{i+1} = \theta_i + h \left( \frac{2835}{27648}k_1 + \frac{18575}{48384}k_3 + \frac{13525}{55296}k_4 + \frac{277}{14336}k_5 + \frac{1}{4}k_6 \right) \quad (51)$$

$$p_{i+1} = p_i + h \left( \frac{2835}{27648}l_1 + \frac{18575}{48384}l_3 + \frac{13525}{55296}l_4 + \frac{277}{14336}l_5 + \frac{1}{4}l_6 \right)$$

where

$$k_1 = f(X_i, \theta_i, p_i)$$

$$l_1 = g(X_i, \theta_i, p_i)$$

$$k_2 = f\left(X_i + \frac{1}{5}h, \theta_i + \frac{1}{5}k_1h, p_i + \frac{1}{5}l_1h\right)$$

$$l_2 = g\left(X_i + \frac{1}{5}h, \theta_i + \frac{1}{5}k_1h, p_i + \frac{1}{5}l_1h\right)$$

$$k_3 = f\left(X_i + \frac{3}{10}h, \theta_i + \frac{3}{40}k_1h + \frac{9}{40}k_2h, p_i + \frac{3}{40}l_1h + \frac{9}{40}l_2h\right)$$

$$k_6 = f\left(X_i + \frac{7}{8}h, \theta_i + \frac{1631}{55296}k_1h + \frac{175}{512}k_2h + \frac{575}{13824}k_3h + \frac{44275}{110592}k_4h + \frac{253}{4096}k_5h, p_i + \frac{1631}{55296}l_1h + \frac{175}{512}l_2h + \frac{575}{13824}l_3h + \frac{44275}{110592}l_4h + \frac{253}{4096}l_5h\right)$$

$$l_6 = g\left(X_i + \frac{7}{8}h, \theta_i + \frac{1631}{55296}k_1h + \frac{175}{512}k_2h + \frac{575}{13824}k_3h + \frac{44275}{110592}k_4h + \frac{253}{4096}k_5h, p_i + \frac{1631}{55296}l_1h + \frac{175}{512}l_2h + \frac{575}{13824}l_3h + \frac{44275}{110592}l_4h + \frac{253}{4096}l_5h\right)$$

$$l_3 = g\left(X_i + \frac{3}{10}h, \theta_i + \frac{3}{40}k_1h + \frac{9}{40}k_2h, p_i + \frac{3}{40}l_1h + \frac{9}{40}l_2h\right)$$

$$k_4 = f\left(X_i + \frac{3}{5}h, \theta_i + \frac{3}{10}k_1h - \frac{9}{10}k_2h + \frac{6}{5}k_3h, p_i + \frac{3}{10}l_1h - \frac{9}{10}l_2h + \frac{6}{5}l_3h\right)$$

$$l_4 = g\left(X_i + \frac{3}{5}h, \theta_i + \frac{3}{10}k_1h - \frac{9}{10}k_2h + \frac{6}{5}k_3h, p_i + \frac{3}{10}l_1h - \frac{9}{10}l_2h + \frac{6}{5}l_3h\right)$$

$$k_5 = f\left(X_i + h, \theta_i - \frac{11}{54}k_1h + \frac{5}{2}k_2h - \frac{70}{27}k_3h + \frac{35}{27}k_4h, p_i - \frac{11}{54}l_1h + \frac{5}{2}l_2h - \frac{70}{27}l_3h + \frac{35}{27}l_4h\right)$$

$$l_5 = g\left(X_i + h, \theta_i - \frac{11}{54}k_1h + \frac{5}{2}k_2h - \frac{70}{27}k_3h + \frac{35}{27}k_4h, p_i - \frac{11}{54}l_1h + \frac{5}{2}l_2h - \frac{70}{27}l_3h + \frac{35}{27}l_4h\right)$$

Using the above fifth-order Runge-Kutta Fehlberg method coupled with shooting method, computer programs are written in MATLAB for the solutions of the Eq. (9). The results for step size,  $h = 0.01$  are presented in the following section.

## 7. Development of an Exact Analytical Solution for the Thermal Model

Exact analytical solution is also developed for the nonlinear thermal model. In doing this, we write

$$\frac{d^2\theta}{dX^2} - Ra\theta^2 - Mc^2\theta - Nr\theta - Ha + Mc^2Q + Mc^2Q\gamma\theta = 0 \quad (53)$$

Using a variable transformation

$$\frac{d\theta}{dX} = \phi \quad (54)$$

One can write that

$$\frac{d^2\theta}{dX^2} = \frac{d\phi}{dX} = \frac{d\theta}{dX} \frac{d\phi}{d\theta} = \phi \frac{d\phi}{d\theta} \quad (55)$$

Putting Eq. (54) and (55) into Eq. (53), results in

$$\phi \frac{d\phi}{d\theta} - Ra\theta^2 - (Mc^2\theta + Nr\theta - Mc^2Q\gamma)\theta + Mc^2Q - H = 0 \quad (56)$$

This can easily be written as

$$\phi d\phi + \{-Ra\theta^2 - Mc^2\theta - Nr\theta - H + Mc^2Q + Mc^2Q\gamma\theta\} d\theta = 0 \quad (57)$$

The above Eq. (57) is a total differential equation which has a solution of the form

$$\frac{1}{2}\phi^2 + Ra(-Mc^2 - Nr - 1)\frac{\theta^3}{3} + \{Mc^2Q\gamma - (Mc^2 - Nr)\}\frac{\theta^2}{2} + Mc^2Q\theta - H\theta = C \quad (58)$$

where  $C$  is the constant of integration Recall that  $\phi = \frac{d\theta}{dX} \rightarrow \phi^2 = \left(\frac{d\theta}{dX}\right)^2$

Therefore, Eq. (58) can be expressed as follows

$$\begin{aligned} &\frac{1}{2}\left(\frac{d\theta}{dX}\right)^2 \\ &+ Ra(-Mc^2 - Nr - 1)\frac{\theta^3}{3} \\ &+ \{Mc^2Q\gamma - (Mc^2 - Nr)\}\frac{\theta^2}{2} \\ &+ Mc^2Q\theta - H\theta = C \end{aligned} \quad (59)$$

Using the first boundary condition,

$$\begin{aligned} X = 1, & \quad \frac{d\theta}{dX} \\ &= 0 \\ &\rightarrow X \\ &= 1, \quad \theta \\ &= \theta_0 \end{aligned}$$

Therefore, the constant  $C$  as

$$\begin{aligned} &Ra(-Mc^2 - Nr - 1)\frac{\theta_0^3}{3} \\ &+ \{Mc^2Q\gamma - (Mc^2 + Nr)\}\frac{\theta_0^2}{2} \\ &+ (Mc^2Q - H)\theta_0 = C \end{aligned} \quad (60)$$

where  $\theta_0$  is the dimensionless temperature at the tip When Eq. (60) is substituted into Eq. (59), we have

$$\begin{aligned} &\frac{1}{2}\left(\frac{d\theta}{dX}\right)^2 \\ &- Ra(-Mc^2 - Nr - 1)\left(\frac{\theta_0^3}{3} - \frac{\theta^3}{3}\right) \\ &+ \{Mc^2Q\gamma - (Mc^2 + Nr)\}\left(\frac{\theta_0^2}{4} - \frac{\theta^2}{4}\right) - (Mc^2Q - H)(\theta_0 - \theta) = 0 \end{aligned} \quad (61)$$

On re-arranging

Eq. (62) is expressed as

$$\begin{aligned} \frac{1}{2} \left( \frac{d\theta}{dX} \right)^2 &= Ra(-Mc^2 - Nr - 1) \left( \frac{\theta_0^3}{3} - \frac{\theta^3}{3} \right) \\ &\quad + (Mc^2Q - H) (\tilde{\theta}_0 - \theta) + \{Mc^2Q\gamma \\ &\quad - (M^2 + Nr)\} \left( \frac{\theta_0^2}{4} - \frac{\theta^2}{4} \right) \\ \sqrt{2}dX &= \frac{d\theta}{\sqrt{\left\{ Ra(Mc^2 + Nr + 1) \left( \frac{\theta^3}{3} - \frac{\theta_0^3}{3} \right) - (Mc^2Q - H) (\theta - \theta_0) - \{Mc^2Q\gamma - (M^2 + Nr)\} \left( \frac{\theta^2}{4} - \frac{\theta_0^2}{4} \right) \right\}}} \end{aligned} \tag{63}$$

Integrating both sides of the Eq. (63), provides

$$\sqrt{2} \int dX = \int \frac{d\theta}{\sqrt{\left\{ Ra(Mc^2 + Nr + 1) \left( \frac{\theta^3}{3} - \frac{\theta_0^3}{3} \right) - (Mc^2Q - H) (\theta - \theta_0) - \{Mc^2Q\gamma - (M^2 + Nr)\} \left( \frac{\theta^2}{4} - \frac{\theta_0^2}{4} \right) \right\}}} \tag{64}$$

$$\sqrt{2}X = \int \frac{d\theta}{\sqrt{\left\{ Ra(Mc^2 + Nr + 1) \left( \frac{\theta^3}{3} - \frac{\theta_0^3}{3} \right) - (Mc^2Q - H) (\theta - \theta_0) - \{Mc^2Q\gamma - (M^2 + Nr)\} \left( \frac{\theta^2}{4} - \frac{\theta_0^2}{4} \right) \right\}}} + C_* \tag{65}$$

Where the arbitrary constant  $C_*$  is found from

$$X = 0, \quad \frac{d\theta}{dX} = 0 \quad \rightarrow \theta = \theta_e \tag{66}$$

suppose that

$$\begin{aligned} G(\theta; Ra, Mc, H, Q, \theta_0) &= G(\theta; Ra, N, Q_h, \theta_0) \\ &= \int \frac{d\theta}{\sqrt{\left\{ Ra(Mc^2 + Nr + 1) \left( \frac{\theta^3}{3} - \frac{\theta_0^3}{3} \right) - (Mc^2Q - H) (\theta - \theta_0) - \{Mc^2Q\gamma - (M^2 + Nr)\} \left( \frac{\theta^2}{4} - \frac{\theta_0^2}{4} \right) \right\}}} \end{aligned} \tag{67}$$

where

$$N = Mc^2 + Nr, \quad Q_h = Mc^2Q - H \tag{68}$$

The integral in Eq. (67) is expressible (e.g. via Wolfram's Mathematica) in term of incomplete elliptic integrals of the first kind. For instant

$$G(\theta; 1, 1, 1, \theta_0) = \sqrt{\frac{\alpha_1^2}{3 + 6\theta_0 + \alpha_1}} \left\{ \frac{\left[ \begin{aligned} &\sqrt{\frac{3 + 6\theta_0 + \alpha_1}{\alpha_1}} \sqrt{\frac{-3 - 6\theta_0 + \alpha_1}{\alpha_1}} \text{EllipticF} \left( \sqrt{\frac{3 + 6\theta_0 + \alpha_1}{2\alpha_1}}, \sqrt{\frac{2\alpha_1}{3 + 6\theta_0 + \alpha_1}} \right) \alpha_2 \\ &- 3 \sqrt{\frac{3 + 2\theta_0 + \alpha_1 + 4\theta}{\alpha_1}} \sqrt{\theta_0 - \theta} \sqrt{\frac{-3 - 2\theta_0 + \alpha_1 + 4\theta}{\alpha_1}} \text{EllipticF} \left( \sqrt{\frac{3 + 2\theta_0 + \alpha_1 + 4\theta}{2\alpha_1}}, \sqrt{\frac{2\alpha_1}{3 + 6\theta_0 + \alpha_1}} \right) \alpha_3 \end{aligned} \right]}{\alpha_2 \alpha_3} \right\} \tag{69}$$

where

$$\alpha_1 = \sqrt{57 - 12\theta_o - 12\theta_o^2}$$

$$\alpha_2 = \sqrt{6\theta^3 - 18\theta + 9\theta^2 - 6\theta_o^3 + 18\theta_o - 9\theta_o^2}$$

$$\alpha_3 = \sqrt{2 - 2\theta_o - 2\theta_o^2}$$

Therefore, the closed-form solution of Eq. (15) can be implicitly expressed as

$$X = G(\theta; Ra, N, Q_h, \theta_o) \tag{70}$$

It should be stated that the unknown  $\theta_0$  in the closed-form solution is found from the following boundary condition. This means that for any given  $N$ ,  $Ra$  and  $Q$ ,  $\theta_0$  is obtained from

$$G(1; Ra, N, Q_h, \theta_o) = 0 \tag{71}$$

With the aid of Wolfram’s Mathematica, the computations of the function  $G(\theta; Ra, N, Q_h, \theta_o)$  are carried out.

## 8. Thermal Efficiency of the fin

The fin efficiency is the ratio of the heat transfer rate by the extended surface to the rate of heat transfer that would be if the entire extended surface were at the base temperature and is given by. With the application of the adimensional variables in Eq. (10), Eq. (72) becomes Eq. (73) can be expressed as

$$\eta = \frac{S_h \int_0^1 \theta^2 dX + \{M^2 + Nr\} \int_0^1 \theta dX + H}{S_h + M^2 + Nr + H} \tag{72}$$

## 9. Results and Discussion

The OHAM solutions are simulated for the purpose of graphical illustrations, sensitivity and parametric investigations. Table 1 presents the

verifications of results of the OHAM of order 1, numerical method (NM) and differential transformation method (DTM). Although, the DTM provides higher accurate results than OHAM as compared to the results of NM and exact analytical solutions. The higher accuracy is due to the large number of terms (18 terms) in the solutions of DTM as compared to the small number of terms (2 terms) in OHAM. This proves that OHAM is a very convenient mathematical method with high convergence rate for the analysis of the nonlinear models. DTM provides simple analytical procedures with high accuracy. However, homotopy analysis method gives the freedom of choosing the best auxiliary parameter that could be used to adjust and control the convergence of the series solution. Such freedom of choice is not offered in the other approximate analytics methods.

The significance of various parameters of the nonlinear model on the thermal management enhancement of thermal systems using the solutions presented are graphical represented for pictorial discussion in Figs. 2-11. The results illustrate that the augmentations of the conductive-radiative, conductive-convective, porosity and magnetic field cause the extended surface adimensional temperature to reduce as a result of increased rate of heat flow via the passive device. The graphical illustrations show that the efficiency and effectiveness of the fin is high at low values of the radiative-conductive, convective-conductive, porosity and magnetic field parameters.

The impacts of convective-conductive, radiative-conductive and porosity parameters on the adimensional temperature distribution in the passive device is graphically illustrated in Fig. 2. The figure shows that as the convection-radiative increases the adimensional temperature in the fin increases. This also means that the local temperature in the extended surface increases as the conduction-convection parameter increases.

It is presented in Fig. 3 about the impact of porosity on the extended surface temperature behaviour. The graphical illustrations show that the amplification of parameter of porosity (Rayleigh number) causes the passive device

**Tab. 1:** Comparative of results via OHAM with DTM and NUM for  $\theta(X)$  when  $Rd = 0.5, \epsilon = 0.1, Ra = 0.4, Nc = 0.3, Nr = 0.2, H = 0.1$ .

X	NUM	DTM	OHAM	HAM	Exact
0.0	0.86349923	0.86349915	0.86349987	0.86349966	0.86349907
0.1	0.86481708	0.86481703	0.86481420	0.86481754	0.86481693
0.2	0.86877626	0.86877619	0.86877319	0.86877671	0.86877611
0.3	0.87539340	0.87539333	0.87539383	0.87539386	0.87539328
0.4	0.88469650	0.88469643	0.88469975	0.88469697	0.88469639
0.5	0.89672509	0.89672504	0.89672757	0.89672557	0.89672497
0.6	0.91153065	0.91153060	0.91152929	0.91153112	0.91153054
0.7	0.92917705	0.92917701	0.92917206	0.92917749	0.92917693
0.8	0.94974120	0.94974116	0.94973660	0.94974156	0.94974112
0.9	0.97331376	0.97331372	0.97331485	0.97331396	0.97331368
1.0	1.00000000	1.00000000	1.00000741	1.00000000	1.00000000

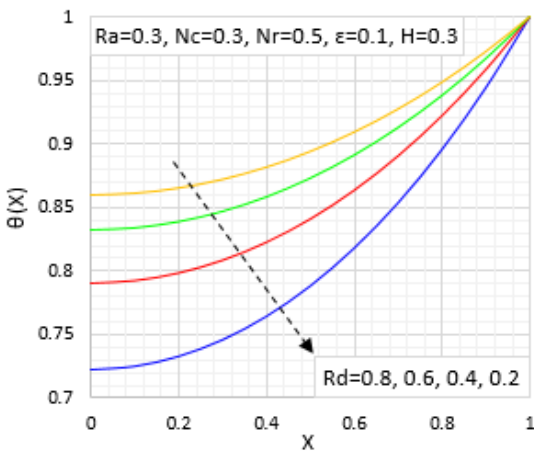


**Fig. 2:** Effects of conductive-radiative on the temperature distribution.

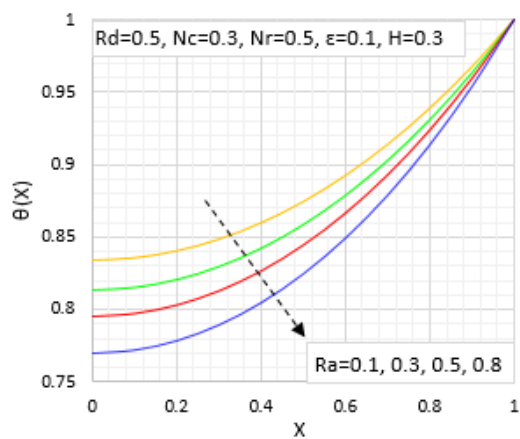


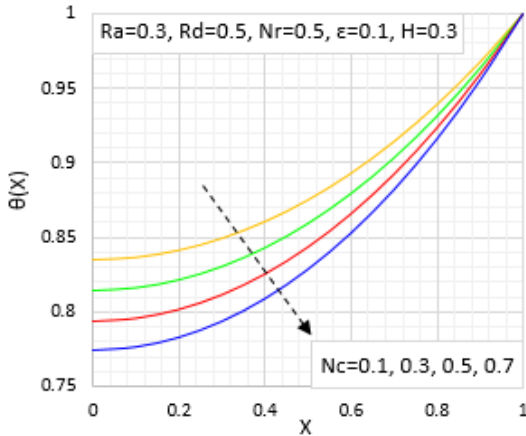
**Fig. 3:** Effects of porous parameter on the temperature distribution.

temperature to be lessened because of the increased permeability allowed by the fin.

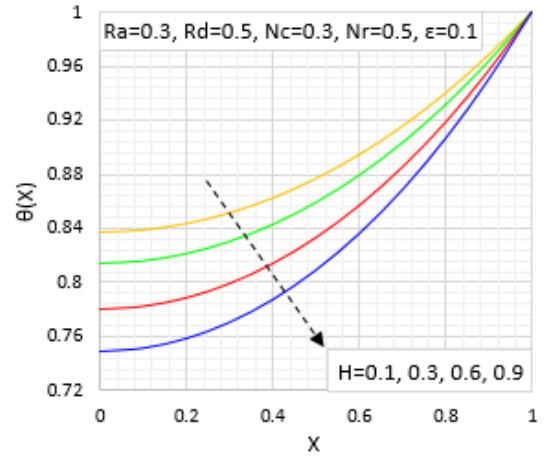
Figs. 4 and 5 display the effects of convective-conductive and radiative-conductive parameters on the fin temperature behaviour. It is shown that the rise of the conductive-radiative, and conductive-convective cause the extended surface adimensional temperature to fall as a result of increased rate of heat flow via the fin. The graphical illustrations show that the efficiency and effectiveness of the fin is high at low values of the radiative-conductive, convective-conductive, porosity and magnetic field parameters.

Fig. 6 displays the effect of value of magnetic field or Lorentz force on the fin temperature behaviours. It is illustrated that when the value of the parameter of the magnetic field increase, the passive device temperature decrease. The graphical illustrations show that the efficiency and effectiveness of the fin is high at low values of the magnetic field parameters.

The effects of convective-conductive, radiative-conductive, magnetic field and porous parameters on the thermal efficiency of the fin are presented in Figs. 8, 9 and 10 while the effect of porosity or void ratio on the fin thermal efficiency is shown in Fig. 11. It is shown in the figures that when the



**Fig. 4:** Effects of convective parameter on the temperature distribution.



**Fig. 6:** Effects of magnetic parameter on the temperature distribution.

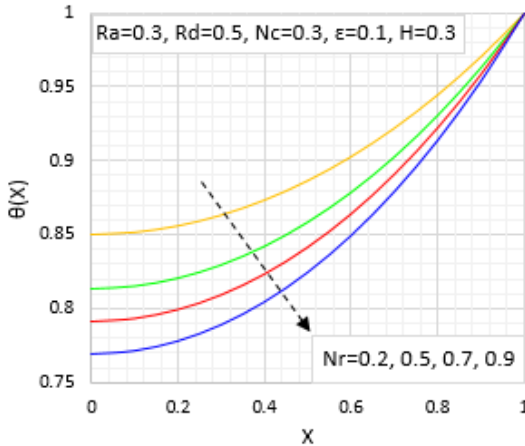


**Fig. 5:** Effects of radiative parameter on the temperature distribution.

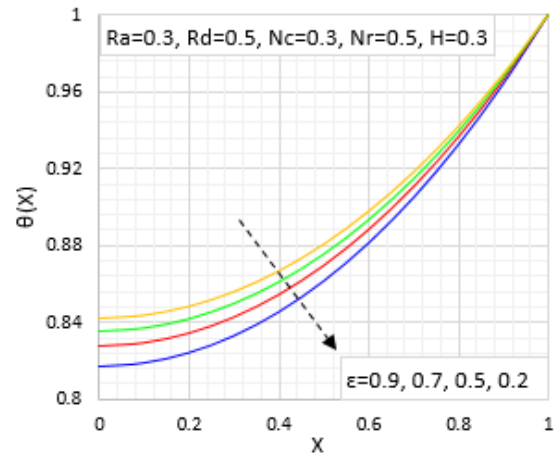


**Fig. 7:** Effects of porosity/void ratio on the temperature distribution.

convective-conductive, radiative-conductive, porosity and magnetic field parameters rise, the passive device efficiency falls.

## 10. Conclusion

This work explored the computational efficiencies and accuracies of three approximate analytical methods; namely, HPM, OHAM and DTM for the nonlinear thermal performance analysis of the convective-radiative porous fin with temperature-dependent internal heat generation

under the influence of magnetic field. The optimal homotopy asymptotic method is shown to be a very convenient mathematical method with high convergence rate. Also, differential transformation method provides simple analytical procedures with high accuracy. However, homotopy analysis method gives the freedom of choosing the best the auxiliary parameter that could be used to adjust and control the convergence of the series solution. Such freedom of choice is not offered in the other approximate analytics methods. The effect of various parameters of the nonlinear model on the thermal

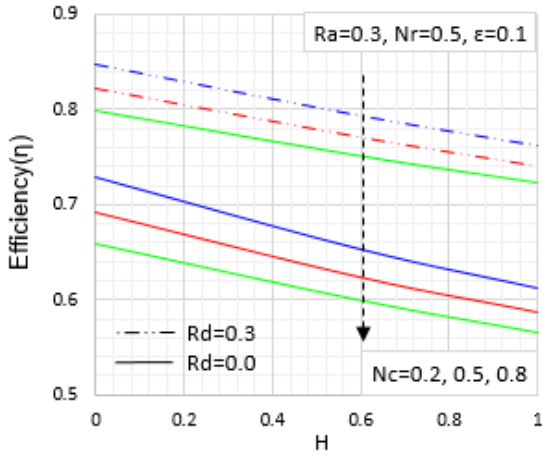


Fig. 8: Effects of convective parameter on the thermal efficiency.

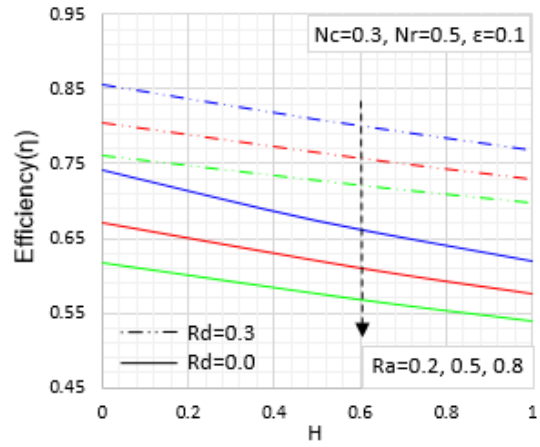


Fig. 10: Effects of porous parameter on the temperature distribution.

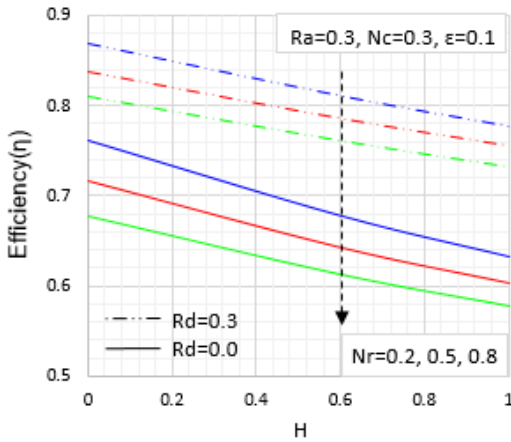


Fig. 9: Effects of radiative parameter on the thermal efficiency.

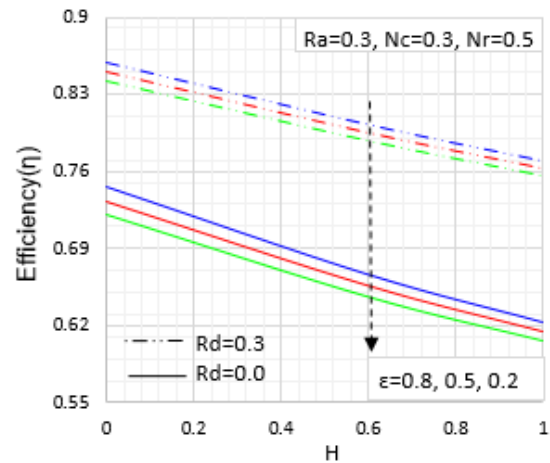


Fig. 11: Effects of porosity/void ratio on the temperature distribution.

management enhancement of thermal systems have been explored using the solutions presented by the method. The graphical representations of the thermal behaviour of the extended surfaces have been presented and the results have been discussed. The study has showed that the augmentations of the conductive-radiative, conductive-convective, porosity and magnetic field cause the extended surface temperature to reduce as a result of increased rate of heat flow via the passive device. The graphical illustrations show that the efficiency and effectiveness of the fin is high at low values of the radiative-conductive, convective-conductive, porosity and

magnetic field parameters. This study will assist in proper thermal analysis of fins and in the design of passive device.

## Nomenclature

$A_{cr}$  Area of the fin cross sections,  $m^2$

$B_o$  magnetic field intensity, Tesla or  $kg/see^2Amp$

$c_{pa}$  specific heat capacity,  $J/kgK$

$h$  coefficient of convective heat transfer,  $W/m^2K$   
 $J_c$  conduction current intensity, A  
 $k$  fin thermal conductivity,  $W/mK$   
 $k_b$  fin thermal conductivity at the base temperature,  $W/mK$   
 $L$  fin length, M  
 $Mc$  adimensional convective parameter  
 $Nr$  adimensional radiation parameter  
 $P$  fin perimeter, m  
 $t$  time, sec.  
 $T$  fin temperature, K  
 $T_\infty$  ambient temperature, K  
 $T_b$  fin temperature at the base, K  
 $x$  fin axial distance, m  
 $X$  adimensional fin length

## Greek Symbols

$\delta$  fin thickness, m  
 $\theta$  adimensional temperature  
 $\theta_b$  adimensional temperature at the fin base  
 $\rho$  fin material density,  $kg/m^3$   
 $\sigma$  Stefan-Boltzmann constant,  $W/m^2K^4$   
 $\sigma$  Electrical conductivity,  $\Omega^{-1}m^{-1}$  or  $sec^2Amp^2/kgm^3$

## References

- [1] Kiwan, S. & Al-Nimr, M. (2001). Using porous fins for heat transfer enhancement. *J Heat Transfer*, 123(4), 790–795.
- [2] Kiwan, S. (2007). Effect of radiative losses on the heat transfer from porous fins. *International Journal of Thermal Sciences*, 46(10), 1046–1055.
- [3] Kiwan, S. & Zeitoun, O. (2008). Natural convection in a horizontal cylindrical annulus using porous fins. *International Journal of Numerical Methods for Heat & Fluid Flow*, 18(5), 618.
- [4] Kiwan, S. (2007). Thermal analysis of natural convection porous fins. *Transport in porous media*, 67, 17–29.
- [5] Gorla, R.S.R. & Bakier, A. (2011). Thermal analysis of natural convection and radiation in porous fins. *International Communications in Heat and Mass Transfer*, 38(5), 638–645.
- [6] Kundu, B., Bhanja, D., & Lee, K.S. (2012). A model on the basis of analytics for computing maximum heat transfer in porous fins. *International Journal of Heat and Mass Transfer*, 55(25-26), 7611–7622.
- [7] Darvishi, M.T., Gorla, R.S.R., Khani, F., & Aziz, A. (2015). Thermal performance of a porous radial fin with natural convection and radiative heat losses. *Thermal Science*, 19(2), 669–678.
- [8] Jordan, A., Khaldi, S., Benmouna, M., & Borucki, A. (1987). Study of non-linear heat transfer problems. *Revue de physique appliquée*, 22(1), 101–105.
- [9] Kundu, B. & Das, P. (2002). Performance analysis and optimization of straight taper fins with variable heat transfer coefficient. *International journal of heat and mass transfer*, 45(24), 4739–4751.
- [10] Khani, F., Raji, M.A., & Nejad, H.H. (2009). Analytical solutions and efficiency of the nonlinear fin problem with temperature-dependent thermal conductivity and heat transfer coefficient. *Communications in Nonlinear Science and Numerical Simulation*, 14(8), 3327–3338.
- [11] Amirkolei, S. & Ganji, D. (2014). Thermal performance of a trapezoidal and rectangular profiles fin with temperature-dependent heat transfer coefficient, thermal conductivity and emissivity. *Indian Journal of Scientific Research*, 1(2), 223–229.

- [12] Aziz, A. & Bouaziz, M. (2011). A least squares method for a longitudinal fin with temperature dependent internal heat generation and thermal conductivity. *Energy conversion and Management*, 52(8-9), 2876–2882.
- [13] Sobamowo, M. (2016). Thermal analysis of longitudinal fin with temperature-dependent properties and internal heat generation using Galerkin's method of weighted residual. *Applied Thermal Engineering*, 99, 1316–1330.
- [14] Ganji, D., Rahgoshay, M., Rahimi, M., & Jafari, M. (2010). Numerical investigation of fin efficiency and temperature distribution of conductive, convective and radiative straight fins. *Int J Res Rev Appl Sci*, 4(3), 230–237.
- [15] Sobamowo, M., Kamiyo, O., & Adeleye, O. (2017). Thermal performance analysis of a natural convection porous fin with temperature-dependent thermal conductivity and internal heat generation. *Thermal Science and Engineering Progress*, 1, 39–52.
- [16] Sobamowo, G.M. (2017). Thermal performance and optimum design analysis of fin with variable thermal conductivity using double decomposition method. *Journal of Mechanical Engineering and Technology (JMETS)*, 9(1), 1–32.
- [17] Sobamowo, G., Jayesimi, L., & Femi-Oyetero, J. (2017). Heat transfer study in a convective-radiative fin with temperature-dependent thermal conductivity and magnetic field using variation parameters method. *Journal of Applied Mathematics and Computational Mechanics*, 16(3), 85–96.
- [18] Moradi, A. & Ahmadikia, H. (2010). Analytical solution for different profiles of fin with temperature-dependent thermal conductivity. *Mathematical Problems in Engineering*, 2010.
- [19] Sadri, S., Raveshi, M.R., & Amiri, S. (2012). Efficiency analysis of straight fin with variable heat transfer coefficient and thermal conductivity. *Journal of Mechanical Science and Technology*, 26, 1283–1290.
- [20] Ndlovu, P.L. & Moitsheki, R.J. (2013). Analytical solutions for steady heat transfer in longitudinal fins with temperature-dependent properties. *Mathematical Problems in Engineering*, 2013.
- [21] Mosayebidorcheh, S., Ganji, D., & Farzinpour, M. (2014). Approximate solution of the nonlinear heat transfer equation of a fin with the power-law temperature-dependent thermal conductivity and heat transfer coefficient. *Propulsion and Power Research*, 3(1), 41–47.
- [22] Ghasemi, S.E., Hatami, M., & Ganji, D. (2014). Thermal analysis of convective fin with temperature-dependent thermal conductivity and heat generation. *Case Studies in Thermal Engineering*, 4, 1–8.
- [23] Ganji, D. & Dogonchi, A. (2014). Analytical investigation of convective heat transfer of a longitudinal fin with temperature-dependent thermal conductivity, heat transfer coefficient and heat generation. *International Journal of Physical Sciences*, 9(21), 466–474.
- [24] Sobamowo, G., Adeleye, O., & Yinusa, A. (2017). Analysis of convective-radiative porous fin With temperature-dependent internal heat Generation and magnetic field using Homotopy Perturbation method. *Journal of computational and Applied Mechanics*, 12(2), 127–145.
- [25] Arslanturk, C. (2010). Optimization of straight fins with a step change in thickness and variable thermal conductivity by homotopy perturbation method. *Journal of Thermal Science and Technology*, 30(2), 9–19.
- [26] Ganji, D.D., Ganji, Z.Z., & Ganji, D.H. (2011). Determination of temperature distribution for annular fins with temperature dependent thermal conductivity by HPM. *Thermal science*, 15(suppl. 1), 111–115.

- [27] Hoshyar, H.A., Rahimpetroudi, I., Ganji, D.D., & Majidian, A.R. (2015). Thermal performance of porous fins with temperature-dependent heat generation via the homotopy perturbation method and collocation method. *Journal of Applied Mathematics and Computational Mechanics*, 14(4), 53–65.
- [28] Haley, K. & Westwater, J. (1966). Boiling heat transfer from single fins. In *International Heat Transfer Conference Digital Library*, Begel House Inc.
- [29] Lai, F.S. & Hsu, Y.Y. (1967). Temperature distribution in a fin partially cooled by nucleate boiling. *AIChE Journal*, 13(4), 817–821.
- [30] Kraus, A.D. (1988). Sixty-Five Years of Extended Surface Technology (1922–1987). *Applied Mechanics Reviews*, 41(9), 321–364.
- [31] Liaw, S. & Yeh, R. (1994). Fins with temperature dependent surface heat flux—I. Single heat transfer mode. *International Journal of Heat and Mass Transfer*, 37(10), 1509–1515.
- [32] Liaw, S. & Yeh, R. (1994). Fins with temperature dependent surface heat flux—II. Multi-boiling heat transfer. *International Journal of Heat and Mass Transfer*, 37(10), 1517–1524.
- [33] Ünal, H. (1985). Determination of the temperature distribution in an extended surface with a non-uniform heat transfer coefficient. *International journal of heat and mass transfer*, 28(12), 2279–2284.
- [34] Ünal, H. (1985). Determination of the temperature distribution in an extended surface with a non-uniform heat transfer coefficient. *International journal of heat and mass transfer*, 28(12), 2279–2284.
- [35] Ünal, H. (1986). A simple method of dimensioning straight fins for nucleate pool boiling. *International journal of heat and mass transfer*, 29(4), 640–644.
- [36] Ünal, H. (1987). An analytic study of boiling heat transfer from a fin. *International journal of heat and mass transfer*, 30(2), 341–349.
- [37] Yeh, R. & Liaw, S. (1990). An exact solution for thermal characteristics of fins with power-law heat transfer coefficient. *International communications in heat and mass transfer*, 17(3), 317–330.
- [38] SEN, A. & TRINH, S. (1986). An exact solution for the rate of heat transfer from a rectangular fin governed by a power law-type temperature dependence. *Journal of heat transfer*, 108(2), 457–459.
- [39] Liaw, S. & Yeh, R. (1990). Analysis of pool boiling heat transfer on a single cylindrical fin. *J Chin Soc Mech Eng*, 11, 448–454.
- [40] Yeh, R. & Liaw, S. (1990). Theoretical study of a fin subject to various types of heat transfer. *Tatung Journal*, 20, 59–66.
- [41] Lin, W. & Lee, D. (1996). Boiling on a straight pin fin. *AIChE journal*, 42(10), 2721–2728.
- [42] Lin, W. & Lee, D. (1996). Experimental study on pin fin boiling. *Heat Transfer Science and Technology*, Ed BX Wang, Higher Education Pub Beijing.
- [43] Ünal, H. (1987). An analytic study of boiling heat transfer from a fin. *International journal of heat and mass transfer*, 30(2), 341–349.
- [44] Lin, W. & Lee, D. (1999). Boiling on a straight pin fin with variable thermal conductivity. *Heat and Mass Transfer*, 34(5), 381–386.
- [45] Sobamowo, M., Ibrahim, S., & Salami, M. (2020). A Study on Thermal Performance of Palladium as Material for Passive Heat Transfer Enhancement Devices in Thermal and Electronics Systems. *Semiconductor Science and Information Devices*, 2(2), 15–24.
- [46] Khani, F., Raji, M.A., & Nejad, H.H. (2009). Analytical solutions and efficiency of the nonlinear fin problem with

temperature-dependent thermal conductivity and heat transfer coefficient. *Communications in Nonlinear Science and Numerical Simulation*, 14(8), 3327–3338.

[47] Liao, S. (2003). *Beyond perturbation: introduction to the homotopy analysis method*. CRC press.